




Surface Electromagnetic Waves near a Black Hole Event Horizon and Their Observational Consequences

Igor I. Smolyaninov 

ECE Department, University of Maryland, College Park, MD 20740, USA; smoly@umd.edu

Abstract: Localization phenomena in light, scattering from random fluctuations of matter fields and space–time metrics near a black hole horizon, were predicted to produce a pronounced peak in the angular distribution of second-harmonic light in the direction normal to the horizon. Therefore, the detection of second-harmonic generation may become a viable observational tool to study spacetime physics near event horizons of astronomical black holes. The light localization phenomena near the horizon may be facilitated by the existence of surface electromagnetic wave solutions. In this communication, we study such surface electromagnetic wave solutions near the horizon of a Schwarzschild metric, describing a black hole in vacuum. We demonstrate that such surface wave solutions must appear when quantum gravity effects are taken into account. Potential observational evidence of this effect is also discussed.

Keywords: surface electromagnetic wave; black hole; second-harmonic generation



Citation: Smolyaninov, I.I. Surface Electromagnetic Waves near a Black Hole Event Horizon and Their Observational Consequences. *Astronomy* **2022**, *1*, 49–57. <https://doi.org/10.3390/astronomy1010006>

Academic Editor: Ignatios Antoniadis

Received: 12 May 2022

Accepted: 3 June 2022

Published: 7 June 2022

Publisher's Note: MDPI stays neutral with regard to jurisdictional claims in published maps and institutional affiliations.



Copyright: © 2022 by the author. Licensee MDPI, Basel, Switzerland. This article is an open access article distributed under the terms and conditions of the Creative Commons Attribution (CC BY) license (<https://creativecommons.org/licenses/by/4.0/>).

1. Introduction

During the recent several years, enormous progress has been made in the imaging and exploration of spatial regions located very near the event horizons of known astronomical black holes [1–3]. However, many more experimental tools will be required in the future to observe and study the complicated physics of these highly non-trivial spacetime regions in more detail. In this communication, we will concentrate on the further development of a recent proposal [4] to use optical second-harmonic (SH) generation as an alternative observational tool to explore gravitational physics in the immediate vicinity of an event horizon of a black hole. In ref. [4], it was demonstrated that SH generation must be strongly enhanced when light from a distant star interacts with random fluctuations of various fields (such as matter fields and fluctuating spacetime metrics) near an event horizon. This strongly directional SH emission occurs due to localization phenomena in light scattering from these fluctuations. It is directed away from the black hole perpendicular to the horizon, and therefore it has a very good chance of escaping from the black hole. As illustrated in Figure 1, this effect resembles the enhancement of SH radiation from randomly rough metal surfaces, which also occurs in the normal direction on a metal surface [5,6]. The SH peak in the normal direction occurs under external spatially coherent irradiation at any illumination direction, provided that the randomly rough surface is capable of supporting surface electromagnetic waves. When an external light source of frequency ω illuminates such a random surface, it couples into a system of weakly localized surface electromagnetic modes. Let us consider one of these surface modes which has a momentum k along the interface. Upon surface propagation, this mode will experience a lot of backscattering, leading to the generation of counterpropagating surface modes with momentum approximately equal to $-k$. When these counterpropagating modes of frequency ω interact via any kind of surface optical nonlinearity, they generate 2ω light. Due to momentum conservation, this SH light may only have a nonzero wave vector component in the direction perpendicular to the surface, leading to the observation of the strongly enhanced diffuse SH generation in this direction. According to experimental observations [6], the angular width of this SH peak

can be as small as a few degrees with respect to the mean normal, and its intensity appears to be much larger compared to the diffuse omnidirectional SH background. While potential observability of this very interesting effect has been established in [4], the theoretical consideration in that work was limited only to the case of the Rindler metric, which describes the immediate vicinity of the black hole event horizon. In this communication, we perform a more realistic study of surface electromagnetic wave solutions near the horizon of a Schwarzschild metric, describing a “real” astronomical black hole in vacuum. We demonstrate that surface wave solutions must also appear under these more realistic conditions (especially when quantum gravity effects are taken into account). Potential observational evidence of this effect will be also discussed.

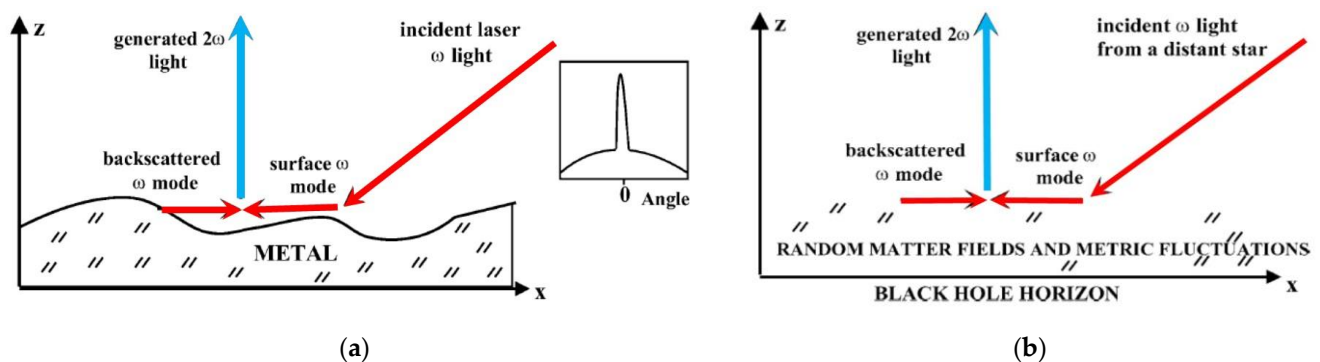


Figure 1. (a) Randomly rough metal surfaces exhibit strongly enhanced SH generation in the direction perpendicular to the surface under illumination with spatially coherent fundamental light. The inset illustrates the typical distribution of the diffuse SH generation with respect to the normal angle to the metal surface. (b) In a similar fashion, SH generation must be strongly enhanced when light from a distant star interacts with random fluctuations of matter fields and spacetime metrics near the event horizon. Escape of the SH light from the black hole is facilitated by the strongly directional character of this effect [4].

2. Results

In order to demonstrate the existence of surface electromagnetic wave solutions near a black hole event horizon, we must solve Maxwell’s Equations in Vacuum in the presence of a gravitational field [7]:

$$\frac{\partial F_{ik}}{\partial x^i} + \frac{\partial F_{li}}{\partial x^k} + \frac{\partial F_{kl}}{\partial x^i} = 0 \quad (1)$$

$$\frac{1}{\sqrt{-g}} \frac{\partial}{\partial x^k} (\sqrt{-g} F^{ik}) = 0 \quad (2)$$

where F_{ik} is the electromagnetic field tensor.

Consideration of electromagnetic wave propagation near a black hole event horizon in [4] was based on the well-known analogy between these Maxwell equations in a curvilinear spacetime metric $g_{ik}(x, t)$ and the macroscopic Maxwell equations describing electromagnetic fields in the presence of matter background with some non-trivial electric permittivity tensor $\epsilon_{ij}(x, t)$ and magnetic permeability tensors $\mu_{ij}(x, t)$ [7]. For example, the equations of electrodynamics in the presence of a static gravitational field look exactly like Maxwell’s equations in some macroscopic electrodynamic medium, in which

$$\epsilon = \mu = g_{00}^{-1/2} \quad (3)$$

where g_{00} is the temporal component of the metric tensor. Following this approach, let us consider the static Schwarzschild metric describing an astronomical black hole in vacuum:

$$ds^2 = \left(1 - \frac{r_s}{r}\right) dt^2 - \frac{dr^2}{\left(1 - \frac{r_s}{r}\right)} - r^2 (d\theta^2 + \sin^2 \theta d\phi^2) \quad (4)$$

where $r_s = 2\gamma M/c^2$ is the Schwarzschild radius of the black hole [7]. The corresponding equivalent material parameters are:

$$\varepsilon = \mu = \frac{1}{\sqrt{1 - \frac{r_s}{r}}} \quad (5)$$

Let us consider solutions of the macroscopic Maxwell equations in such a spherically symmetric geometry. The spatial variables in the Maxwell equations written in the spherical coordinates partially separate, and without the loss of generality we may assume field dependencies proportional to $e^{i(m\phi - \omega t)}$, where m is an integer. The macroscopic Maxwell equations may be written using the spherical coordinates (r, θ, ϕ) as [8]:

$$\frac{1}{r \sin \theta} \left[\frac{\partial}{\partial \theta} (\sin \theta E_\phi) - im E_\theta \right] = \frac{i\omega\mu}{c} H_r \quad (6)$$

$$\frac{im}{r \sin \theta} E_r - \frac{1}{r} \frac{\partial}{\partial r} (r E_\phi) = \frac{i\omega\mu}{c} H_\theta \quad (7)$$

$$\frac{1}{r} \frac{\partial}{\partial r} (r E_\theta) - \frac{1}{r} \frac{\partial E_r}{\partial \theta} = \frac{i\omega\mu}{c} H_\phi \quad (8)$$

$$\frac{1}{r \sin \theta} \left[\frac{\partial}{\partial \theta} (\sin \theta H_\phi) - im H_\theta \right] = -\frac{i\omega\varepsilon}{c} E_r \quad (9)$$

$$\frac{im}{r \sin \theta} H_r - \frac{1}{r} \frac{\partial}{\partial r} (r H_\phi) = -\frac{i\omega\varepsilon}{c} E_\theta \quad (10)$$

$$\frac{1}{r} \frac{\partial}{\partial r} (r H_\theta) - \frac{1}{r} \frac{\partial H_r}{\partial \theta} = -\frac{i\omega\varepsilon}{c} E_\phi \quad (11)$$

$$\frac{1}{r} \frac{\partial}{\partial r} (r^2 \varepsilon E_r) + \frac{\varepsilon}{\sin \theta} \frac{\partial}{\partial \theta} (\sin \theta E_\theta) + \frac{im\varepsilon}{\sin \theta} E_\phi = 0 \quad (12)$$

$$\frac{1}{r} \frac{\partial}{\partial r} (r^2 \mu H_r) + \frac{\mu}{\sin \theta} \frac{\partial}{\partial \theta} (\sin \theta H_\theta) + \frac{im\mu}{\sin \theta} H_\phi = 0 \quad (13)$$

These equations may be simplified if we assume that $m = 0$, which may be achieved for any given light ray by choosing the proper system of coordinates. Moreover, if $m = 0$ the TM and TE polarized solutions may be separated, so that for the TM solutions (for which $E_\phi = H_r = H_\theta = 0$) we obtain:

$$E_r = \frac{ic}{\omega\varepsilon r \sin \theta} \frac{\partial}{\partial \theta} (\sin \theta H_\phi) \quad (14)$$

$$E_\theta = -\frac{ic}{\omega\varepsilon r} \frac{\partial}{\partial r} (r H_\phi) \quad (15)$$

Substitution of Equations (14) and (15) into Equation (8) gives rise to the following wave equation for the TM polarized light:

$$-\frac{\varepsilon}{r} \frac{\partial}{\partial r} \left(\frac{1}{\varepsilon} \frac{\partial}{\partial r} (r H_\phi) \right) - \frac{1}{r^2} \frac{\partial}{\partial \theta} \left(\frac{1}{\sin \theta} \frac{\partial}{\partial \theta} (\sin \theta H_\phi) \right) = \frac{\varepsilon \mu \omega^2}{c^2} H_\phi \quad (16)$$

Let us search for the approximate solutions to Equation (16) which have the following functional form:

$$H_\phi \sim e^{ik_\theta r \theta} \quad (17)$$

where $rk_\theta \gg 1$ is assumed. Under such an assumption, the wave equation may be re-written as:

$$-\frac{\varepsilon}{r} \frac{\partial}{\partial r} \left(\frac{1}{\varepsilon} \frac{\partial}{\partial r} (rH_\phi) \right) - \frac{\varepsilon \mu \omega^2}{c^2} H_\phi = -k_\theta^2 H_\phi \quad (18)$$

which may be recast as a one-dimensional Schrödinger equation for an effective wave function defined as $\psi = H_\phi r / \sqrt{\varepsilon}$:

$$-\frac{\partial^2 \psi}{\partial r^2} + \left(-\frac{1}{2\varepsilon} \frac{\partial^2 \varepsilon}{\partial r^2} + \frac{3}{4\varepsilon^2} \left(\frac{\partial \varepsilon}{\partial r} \right)^2 - \varepsilon \mu \frac{\omega^2}{c^2} \right) \psi = -\frac{\partial^2 \psi}{\partial r^2} + V\psi = -k_\theta^2 \psi \quad (19)$$

In the latter equation, V plays the role of an effective potential and $-k_\theta^2$ plays the role of a total energy. Based on the expression for ε and μ from Equation (5), the effective potential near a Schwarzschild black hole equals

$$V = -\frac{\omega^2}{c^2} \frac{1}{\left(1 - \frac{r_s}{r}\right)} - \frac{r_s \left(1 - \frac{r_s}{4r}\right)}{2r^3 \left(1 - \frac{r_s}{r}\right)^2} + \frac{3r_s^2}{16r^4 \left(1 - \frac{r_s}{r}\right)^2} \approx -\frac{\omega^2 r_s}{c^2 \rho} - \frac{3}{16\rho^2} \quad (20)$$

where we have assumed that $r = r_s + \rho$ and $\rho \ll r_s$. This potential (plotted schematically in Figure 2) appears to be real and well-behaved even below the horizon, even though the effective ε and μ parameters themselves are imaginary (as defined by Equation (5)). Moreover, as noted in [4], the divergence of this potential at $\rho = 0$ is supposed to be tamed by the quantum gravity effects. Note that such a situation is not unusual in macroscopic electrodynamics. A similar situation is observed in the recently discovered surface electromagnetic waves guided by strongly lossy gradient structures [9]. We should also mention that the spacetime metric of a black hole interior is typically obtained as an analytical continuation of the conventional Schwarzschild metric (Equation (4)) above the horizon, in which the dynamical roles of the temporal and radial coordinates are interchanged [10]. It is easy to verify that such an exchange does not affect Equations (1) and (2). Therefore, the effective potential described by Equation (20) appears to be reasonably well justified.

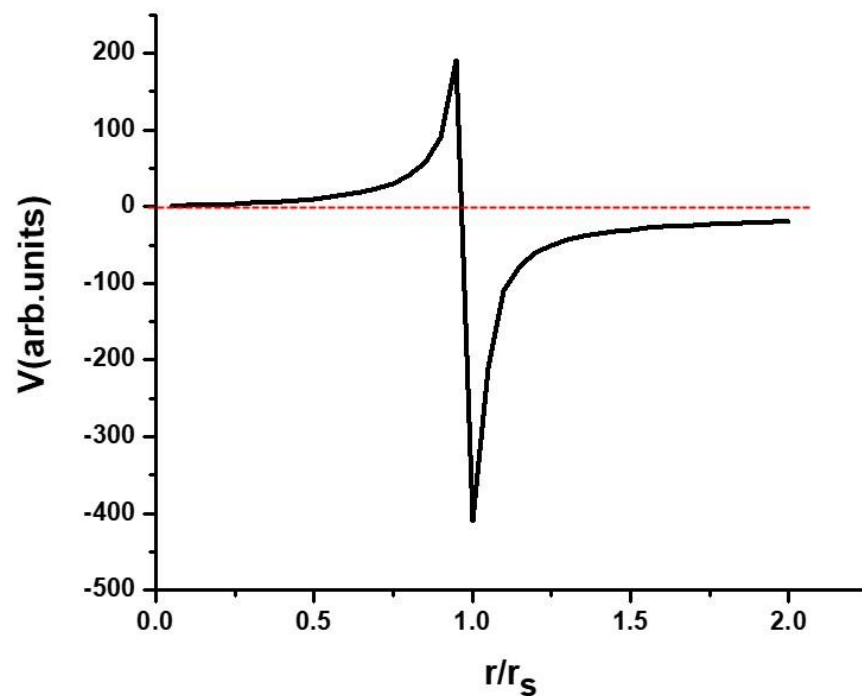


Figure 2. Basic shape of the effective potential from Equation (20) near the horizon.

Let us analyze the eigenstate solutions of this effective Schrodinger equation. We should note that very near the horizon, the potential energy term proportional to $1/\rho^2$ will always dominate. However, this only happens at very short distances when

$$\rho < \frac{3\lambda^2}{64\pi^2 r_s} \quad (21)$$

where λ is the wavelength of light at infinity. At larger distances, the effective potential is Coulomb-like. An extensive analysis of solutions of the Schrödinger equation with a “Coulomb plus inverse-square potential”

$$V = -\frac{B}{\rho} + \frac{A}{\rho^2} \quad (22)$$

may be found in [11]. If $A > -1/8$, the energy eigenstates of this potential are:

$$E(n) = -\frac{2B^2}{\left(2n - 1 + \sqrt{1 + 8A}\right)^2} \quad (23)$$

In contrast, if $A < -1/8$, the ρ -component of the spatial frequency diverges near $\rho = 0$, and there is no finite ground state (the particle falls into the horizon). Since in our case $A = -3/16 < -1/8$ (see Equation (20)), we have obtained a familiar conclusion that there are no zero-geodesics near the surface of a black hole within the scope of classical treatment of the Schwarzschild metric. In the absence of quantum gravity effects, every photon falls towards the horizon, and it is inevitably absorbed by the black hole. However, based on the general properties of the 1D Schrödinger equations [12], it is well-known that the case of $1/\rho^2$ potential is a borderline case, which separates potential wells exhibiting finite ground energy states from the much more divergent potential wells in which a finite ground state may not exist. In particular, any potential well that is weaker than $1/\rho^2$ exhibits a finite ground state. Therefore, the emergence of a cutoff for any particular reason in the divergent $1/\rho^2$ behavior of the potential $V(\rho)$ near a black hole event horizon (for example, due to the emergence of quantum gravitational minimum length l_{min} of the order of the Planck scale) leads to the emergence of a well-defined ground eigenstate among the wave functions described by Equation (19). This eigenstate, located at $k_\theta \sim l_{min}^{-1}$, gives rise to a fundamental guided surface electromagnetic wave propagating near the horizon. Note that the field configuration and the dispersion law of this mode strongly resemble the charge density wave in a gradient waveguide described in [9]. In addition, a set of well-defined excited surface states will also appear in this limit, which at large n will tend to

$$E(n) = -k_{\theta n}^2 \approx -\frac{B^2}{2n^2} \quad (24)$$

due to the Coulomb-like character of the attractive potential $V(\rho)$ at large ρ . The dispersion law of these excited modes appears to be:

$$k_{\theta n} \approx \frac{\omega^2 r_s}{\sqrt{2} c^2 n} \quad (25)$$

Thus, our detailed consideration reveals a family of surface electromagnetic wave modes near the horizon, which justifies the proposal [4] to use optical SH generation (mediated by these modes) as an observational tool to explore gravitational physics in the immediate vicinity of the horizon.

3. Discussion

The presence of surface electromagnetic wave solutions near the horizon in the more general framework of a Schwarzschild metric further justifies the theory of SH generation near the horizon, which was developed in [4]. This theory is virtually identical to the theory of strongly enhanced directional SH generation from randomly rough metal surfaces [5]. The latter theory was confirmed in the experiments with randomly rough metal surfaces capable of supporting surface electromagnetic waves [6], in which a narrow SH peak in the normal direction was observed under external spatially coherent laser illumination at any illumination direction. This interesting effect appears to be a generic property of systems which support surface electromagnetic modes and exhibit weak disorder. An essential similarity between the surface plasmon geometry described in [5,6] and an astronomical situation in which light from a distant star interacts with a black hole horizon (see Figure 1), arises from the fact that the illuminating light in both cases has a very high degree of spatial coherence. Since photon interference is the root cause of the localization effects in light scattering, such effects are only possible for spatially coherent illumination. Distant stars indeed provide a source of such spatially coherent illumination (which is somewhat similar to laser light) because of their small angular dimensions.

It is also important, however, that SH light directed perpendicular to the event horizon has the most chances to leave the neighborhood of a black hole. As a result, such an SH light may become a dominant component of its visible emission. Indeed, the omnidirectionally scattered fundamental (ω) and SH (2ω) light will be predominantly re-absorbed by the black hole. As a result, for a distant observer, the intensity of the diffuse fundamental and SH light will be substantially attenuated in comparison with the directional second-harmonic peak. While the observation of such an SH emission may not be easy, the described effect may be used to obtain unique experimental information on the inner workings of quantum gravity. Similar to Hawking radiation, the described SH emission is caused by the quantum gravitational effects at very high spatial frequencies (of the order of the Planck scale). On the other hand, localization effects induced by the quantum spacetime fluctuations, which are necessary for the directional SH generation to occur, do not play a substantial role in Hawking radiation. Another important distinction between these two effects is that Hawking radiation is an internal property of a black hole, while the directional SH radiation represents a black hole's reaction to the external illumination. Therefore, the described directional SH generation and Hawking radiation are two very different effects of quantum gravity.

Another potentially interesting consequence of the newly obtained surface electromagnetic wave solutions, which look very similar to the charge density waves in gradient waveguides [9], is that we may potentially assign an interesting direct physical meaning to the holographic principle [13]. According to this guiding principle of quantum gravity, the physical description of a volume of space can be thought of as encoded on a surface bounding this volume, such as a gravitational horizon. As we have seen from Equation (5), from the electromagnetic point of view, a horizon corresponds to a surface where $\epsilon = \mu \rightarrow \infty$, which means that a horizon must act as an electric and magnetic mirror (see Figure 3). For example, an electric charge q located at a distance l from the horizon must induce a redistribution of surface charge density σ on the horizon defined as:

$$\sigma(x, y) = -\frac{ql}{2\pi(x^2 + y^2 + l^2)^{3/2}} \quad (26)$$

and leads to the appearance of an “image charge” in the mirror. As a result, the real volume physics will be dutifully “reflected” by the 2D redistribution of these surface charges. Excitation and propagation of the newly obtained surface charge density waves at the horizon may provide a real physical mechanism behind holographic imaging. Note, however, that a self-force acting on an accelerated charge indeed has a contribution, which

may be interpreted as a Coulomb force from an image charge reflected in a distant Rindler horizon (see for example [14]).

As far as observational consequences of the black hole SH emission are concerned, it may potentially be detected as a weak anomalously blue-shifted light source whose total brightness must be proportional to the surface area of the black hole and the square of the total incident light intensity provided by nearby light sources. Assuming that the optical nonlinearities near the horizon must be extremely strong due to enormous field intensities near the horizon, the second-harmonic conversion efficiency may be considerable (for example, in some solid-state physics situations, SH conversion efficiency reaches up to ~10%). This argument provides reasonably optimistic chances of the detection of SH light generated by a black hole located in a dense stellar association or in a center of a bright galaxy.

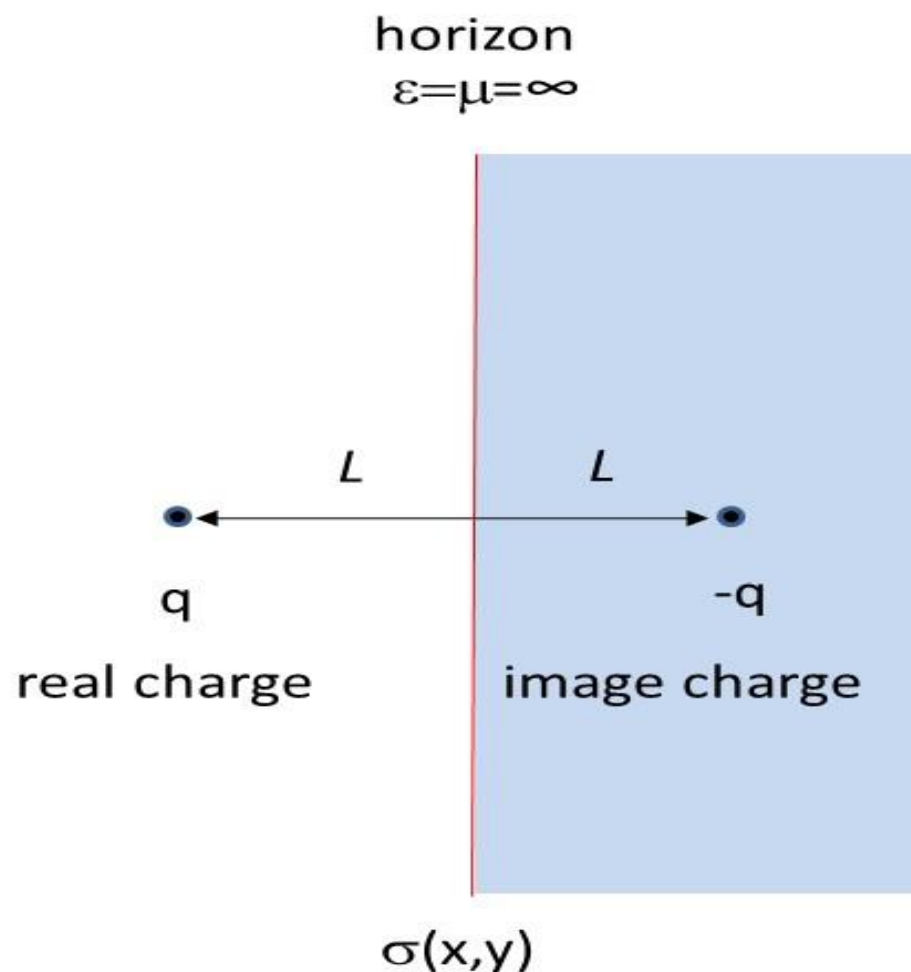


Figure 3. Appearance of image charges reflected in the mirror is caused by propagation and redistribution of surface charges σ .

We should also mention that experimental observations of SH light from various astronomical sources are not unusual. In particular, we can mention observations of SH of the cyclotron line in the spectra of such high-mass bright X-ray sources as 4U1907+09, which were obtained by the BeppoSAX [15]. Since such highly massive bright X-ray sources are widely believed to be powered by black holes, these and similar experimental observations may potentially need to be re-analyzed in search of evidence of the highly interesting quantum gravity effects described above.

Even though it may be difficult to observe these effects in astronomical observations, one might also observe these effects in the higher-dimensional mini-black holes on the Planck mass scale, which would be observed in future accelerator experiments [16]. When the black hole mass approaches the order of the Planck mass due to Hawking radiation, it would be expected that quantum gravity effects would also lead to quantum fluctuations in the background metric. In four dimensions, such modified background geometries would be given by the quantum deformed Schwarzschild black holes [17], the black holes in the noncommutative models [18], and black holes in the asymptotically safe gravity [19].

4. Conclusions

In conclusion, we have demonstrated that localization phenomena in light scattering from random fluctuations of matter fields and quantum spacetime in the vicinity of a black hole horizon may produce an intense peak of second-harmonic light directed perpendicular and away from the horizon. Therefore, detection of second-harmonic generation may become a viable observational tool to study spacetime physics near event horizons of an astronomical black hole. The light localization phenomena near the horizon may be facilitated by the existence of surface electromagnetic wave solutions. Such surface wave solutions must appear when quantum gravity effects are taken into account. Potential observational evidence of this effect has been discussed, which indicates the experimental viability of the proposed technique.

Funding: This research received no external funding.

Institutional Review Board Statement: Not applicable.

Informed Consent Statement: Not applicable.

Data Availability Statement: Not applicable.

Conflicts of Interest: The author declares no conflict of interest.

References

1. Oldham, L.J.; Auger, M.W. Galaxy structure from multiple tracers—II. M87 from parsec to megaparsec scales. *Mon. Not. R. Astron. Soc.* **2016**, *457*, 421–439. [\[CrossRef\]](#)
2. Bouman, K.L.; Johnson, M.D.; Zoran, D.; Fish, V.L.; Doeleman, S.S.; Freeman, W.T. Computational Imaging for VLBI Image Reconstruction. In Proceedings of the IEEE Conference on Computer Vision and Pattern Recognition, Las Vegas, NV, USA, 27–30 June 2016; pp. 913–922.
3. The Event Horizon Telescope Collaboration; Akiyama, K.; Alberdi, A.; Alef, W.; Asada, K.; Azulay, R.; Bacsko, A.; Ball, D.; Baloković, M.; Barrett, J.; et al. First M87 event horizon telescope results. I. The shadow of the supermassive black hole. *Astrophys. J. Lett.* **2019**, *875*, L1. [\[CrossRef\]](#)
4. Smolyaninov, I.I. Optical second harmonic generation near a black hole horizon as possible source of experimental information on quantum gravitational effects. *Phys. Lett. A* **2002**, *300*, 375–380. [\[CrossRef\]](#)
5. McGurn, A.R.; Leskova, T.A.; Agranovich, V.M. Weak-localization effects in the generation of second harmonics of light at a randomly rough vacuum-metal grating. *Phys. Rev. B* **1991**, *44*, 11441. [\[CrossRef\]](#) [\[PubMed\]](#)
6. Aktsipetrov, O.A.; Golovkina, V.N.; Kapusta, O.I.; Leskova, T.A.; Novikova, N.N. Anderson localization effects in the second harmonic generation at a weakly rough metal surface. *Phys. Lett. A* **1992**, *170*, 231–234. [\[CrossRef\]](#)
7. Landau, L.; Lifshitz, E. *The Classical Theory of Fields*; Elsevier: Oxford, UK, 2000.
8. Kulyabov, D.S.; Korolkova, A.V.; Korolkov, V.I. Maxwell's equations in arbitrary coordinate system. *Bull. PFUR Ser. Math. Inf. Sci. Phys.* **2012**, *1*, 96–106.
9. Smolyaninov, I.I. Surface electromagnetic waves at gradual interfaces between lossy media. *PIER* **2021**, *170*, 177–186. [\[CrossRef\]](#)
10. Doran, R.; Lobo, F.S.N.; Crawford, P. Interior of a Schwarzschild black hole revisited. *Found. Phys.* **2008**, *38*, 160–187. [\[CrossRef\]](#)
11. Dong, S.H.; Sun, G.H. The Schrodinger equation with a Coulomb plus inverse-square potential in D dimensions. *Phys. Scr.* **2004**, *70*, 94–97. [\[CrossRef\]](#)
12. Landau, L.D.; Lifshitz, E.M. *Quantum Mechanics*; Pergamon: New York, NY, USA, 1984.
13. Susskind, L. The world as a hologram. *J. Math. Phys.* **1995**, *36*, 6377–6396. [\[CrossRef\]](#)
14. Eriksen, E.; Grøn, Ø. Electrodynamics of hyperbolically accelerated charges V. The field of a charge in the Rindler space and the Milne space. *Ann. Phys.* **2004**, *313*, 147–196. [\[CrossRef\]](#)
15. Cusumano, G.; di Salvo, T.; Burderi, L.; Orlandini, M.; Piraino, S.; Robba, N.; Santangelo, A. Detection of a cyclotron line and its second harmonic in 4U1907+09. *Astron. Astrophys.* **1998**, *338*, L79–L82.

-
16. Koch, B.; Bleicher, M.; Hossenfelder, S. Black hole remnants at the LHC. *JHEP* **2005**, *10*, 053. [[CrossRef](#)]
 17. Kazakov, D.I.; Solodukhin, S.N. On quantum deformation of the Schwarzschild solution. *Nucl. Phys.* **1994**, *B429*, 153–176. [[CrossRef](#)]
 18. Nicolini, P.; Smailagic, A.; Spallucci, E. Noncommutative geometry inspired Schwarzschild black hole. *Phys. Lett. B* **2006**, *632*, 547–551. [[CrossRef](#)]
 19. Bonanno, A.; Reuter, M. Renormalization group improved black hole spacetimes. *Phys. Rev. D* **2000**, *62*, 043008. [[CrossRef](#)]